



IJRASET

International Journal For Research in
Applied Science and Engineering Technology



INTERNATIONAL JOURNAL FOR RESEARCH

IN APPLIED SCIENCE & ENGINEERING TECHNOLOGY

Volume: 12 **Issue:** I **Month of publication:** January 2024

DOI: <https://doi.org/10.22214/ijraset.2024.58011>

www.ijraset.com

Call:  08813907089

E-mail ID: ijraset@gmail.com

Spectral and FTIR Analysis of Ho^{3+} ions doped ZincLithium Potassium Calcium Alumino Borophosphate Glasses

S.L. Meena

Ceramic Laboratory, Department of physics, Jai Narain Vyas University, Jodhpur 342001(Raj) India

Abstract: Glasses samples containing Ho^{3+} in zinc lithium potassium calcium alumino borophosphate glasses $(30-x)\text{P}_2\text{O}_5$: 10ZnO : $10\text{Li}_2\text{O}$: $10\text{K}_2\text{O}$: 10CaO : $10\text{Al}_2\text{O}_3$: $20\text{B}_2\text{O}_3$: $x\text{Ho}_2\text{O}_3$. (where $x=1, 1.5, 2$ mol %) have been prepared by melt-quenching method. The amorphous nature of the prepared glass samples was confirmed by X-ray diffraction. Optical absorption, Excitation, fluorescence and FTIR spectra were recorded at room temperature for all glass samples. Judd-Ofelt intensity parameters Ω_λ ($\lambda=2, 4$ and 6) are evaluated from the intensities of various absorption bands of optical absorption spectra. Using these intensity parameters various radiative properties like spontaneous emission probability (A), branching ratio (β), radiative life time (τ_R) and stimulated emission cross-section (σ_p) of various emission lines have been evaluated.

Keywords: ZLPCABP Glasses, Optical Properties, FTIR Spectroscopy, Judd-Ofelt Theory,

I. INTRODUCTION

Rare earth doped glasses are being extensively studied due to their technological importance and their applications in the field of glass ceramics, thermal sensors and reflecting windows [1-5]. Among different glasses, phosphate glasses are quite prone with the advantages such as low non-linear refractive index, good physical and chemical stability and high transparency from near Ultra Violet to mid-Infrared region [6-9]. Zinc oxide is added in the glass matrix to increase glass forming ability and to ensure low rates of crystallization in the glass system. Phosphate glasses are important materials because they generally offer some unique physical, optical and spectral properties better than other glasses [10-12]. The addition of network modifier (NWF) Li_2O is to improve both electrical and mechanical properties of such glasses. Al_2O_3 is often added to modify the glass structure that improves the physical properties, chemical durability and mechanical strength. Borophosphate glass systems exhibit high refractive indices, high density, high solubility and optical susceptibilities. They present superior properties that include high transparency, low melting point, high thermal stability and high solubility for rare-earth ions and low dispersion [13-15].

The present work reports on the preparation and characterization of rare earth doped heavy metal oxide (HMO) glass systems for lasing materials. I have studied on the Optical absorption, Excitation, fluorescence and FTIR spectra of Ho^{3+} doped zinc lithium potassium calcium alumino borophosphate glasses. The intensities of the transitions for the rare earth ions have been estimated successfully using the Judd-Ofelt theory, The laser parameters such as radiative probabilities(A), branching ratio (β), radiative life time(τ_R) and stimulated emission cross section(σ_p) are evaluated using J.O.intensity parameters(Ω_λ , $\lambda=2, 4$ and 6).

II. EXPERIMENTAL TECHNIQUES

Preparation of Glasses

The following Ho^{3+} doped borophosphate glass samples $(30-x)\text{P}_2\text{O}_5$: 10ZnO : $10\text{Li}_2\text{O}$: $10\text{K}_2\text{O}$: 10CaO : $10\text{Al}_2\text{O}_3$: $20\text{B}_2\text{O}_3$: $x\text{Ho}_2\text{O}_3$. (where $x=1, 1.5$ and 2 mol%) have been prepared by melt-quenching method. Analytical reagent grade chemical used in the present study consist of P_2O_5 , ZnO , Li_2O , K_2O , CaO , Al_2O_3 , B_2O_3 and Ho_2O_3 . They were thoroughly mixed by using an agate pestle mortar. then melted at 1058°C by an electrical muffle furnace for 2h., After complete melting, the melts were quickly poured in to a preheated stainless steel mould and annealed at temperature of 250°C for 2h to remove thermal strains and stresses. Every time fine powder of cerium oxide was used for polishing the samples. The glass samples so prepared were of good optical quality and were transparent. The chemical compositions of the glasses with the name of samples are summarized in **Table 1**.

Table 1.

Chemical composition of the glasses

Sample Glass composition (mol %)

ZLPCABP (UD) 30P₂O₅: 10ZnO: 10Li₂O: 10K₂O: 10CaO: 10Al₂O₃:20B₂O₃

ZLPCABP (HO1) 29P₂O₅: 10ZnO: 10Li₂O: 10K₂O: 10CaO: 10Al₂O₃:20B₂O₃:1 Ho₂O₃

ZLPCABP (HO1.5)28.5P₂O₅: 10ZnO: 10Li₂O: 10K₂O: 10CaO: 10Al₂O₃:20B₂O₃:1.5 Ho₂O₃

ZLPCABP (HO2) 28P₂O₅: 10ZnO: 10Li₂O: 10K₂O: 10CaO: 10Al₂O₃:20B₂O₃:2 Ho₂O₃

ZLPCABP (UD) -Represents undoped Zinc Lithium Potassium Calcium Alumino Borophosphate glass specimens

ZLPCABP (HO)-Represents Ho³⁺ doped Zinc Lithium Potassium Calcium Alumino Borophosphate glass specimens

III. THEORY

A. Oscillator Strength

The intensity of spectral lines are expressed in terms of oscillator strengths using the relation [16].

$$f_{\text{expt.}} = 4.318 \times 10^9 [\epsilon(\nu) d \nu] \quad (1)$$

where, $\epsilon(\nu)$ is molar absorption coefficient at a given energy ν (cm⁻¹), to be evaluated from Beer–Lambert law.

Under Gaussian Approximation, using Beer–Lambert law, the observed oscillator strengths of the absorption bands have been experimentally calculated [17], using the modified relation:

$$P_m = 4.6 \times 10^{-9} \times \frac{1}{cl} \log \frac{I_0}{I} \times \Delta\nu_{1/2} \quad (2)$$

where c is the molar concentration of the absorbing ion per unit volume, l is the optical path length, $\log I_0/I$ is optical density and $\Delta\nu_{1/2}$ is half band width.

B. Judd-Ofelt Intensity Parameters

According to Judd [18] and Ofelt [19] theory, independently derived expression for the oscillator strength of the induced forced electric dipole transitions between an initial J manifold $|4f^N(S, L) J\rangle$ level and the terminal J' manifold $|4f^N(S', L') J'\rangle$ is given by:

$$\frac{8\pi^2 mc \bar{\nu}}{3h(2J+1)n} \left[\frac{(n^2+2)^2}{9} \right] \times S(J, J') \quad \text{Where,} \quad (3)$$

the line strength $S(J, J')$ is given by the equation

$$S(J, J') = e^2 \sum_{\lambda=2, 4, 6} \Omega_{\lambda} \langle 4f^N(S, L) J || U^{(\lambda)} || 4f^N(S', L') J' \rangle^2 \quad (4)$$

In the above equation m is the mass of an electron, c is the velocity of light, $\bar{\nu}$ is the wave number of the transition, h is Planck's constant, n is the refractive index, J and J' are the total angular momentum of the initial and final level respectively, Ω_{λ} ($\lambda=2, 4$ and 6) are known as Judd-Ofelt intensity.

C. Radiative Properties

The Ω_{λ} parameters obtained using the absorption spectral results have been used to predict radiative properties such as spontaneous emission probability (A) and radiative life time (τ_R), and laser parameters like fluorescence branching ratio (β_R) and stimulated emission cross section (σ_p).

The spontaneous emission probability from initial manifold $|4f^N(S', L') J'\rangle$ to a final manifold $|4f^N(S, L) J\rangle$ is given by:

$$A[(S', L') J'; (S, L) J] = \frac{64 \pi^2 \bar{\nu}^3}{3h(2J'+1)} \left[\frac{n(n^2+2)^2}{9} \right] \times S(J', J) \quad (5)$$

$$\text{Where, } S(J', J) = e^2 [\Omega_2 || U^{(2)} ||^2 + \Omega_4 || U^{(4)} ||^2 + \Omega_6 || U^{(6)} ||^2]$$

The fluorescence branching ratio for the transitions originating from a specific initial manifold $|4f^N(S', L') J'\rangle$ to a final manifold $|4f^N(S, L) J\rangle$ is given by

$$\beta[(S', L') J'; (S, L) J] = \frac{A[(S', L') J'; (S, L) J]}{\sum_{S' L' J'} A[(S', L') J'; (S', L') J']} \quad (6)$$

S L J

where, the sum is over all terminal manifolds.

The radiative life time is given by

$$\tau_{rad} = \sum_{S L J} A[(S', L') J'; (S, L)] = A_{Total}^{-1} \quad (7)$$

S L J

where, the sum is over all possible terminal manifolds. The stimulated emission cross-section for a transition from an initial manifold $|4f^N(S', L') J\rangle$ to a final manifold $|4f^N(S, L) J\rangle$ is expressed as

$$\sigma_p(\lambda_p) = \left[\frac{\lambda_p^4}{8\pi c n^2 \Delta\lambda_{eff}} \right] \times A[(S', L') J'; (\bar{S}, \bar{L}) \bar{J}] \quad (8)$$

where, λ_p the peak fluorescence wavelength of the emission band and $\Delta\lambda_{eff}$ is the effective fluorescence line width.

D. Nephelauxetic Ratio (β') and Bonding Parameter ($b^{1/2}$)

The nature of the R-O bond is known by the Nephelauxetic Ratio (β') and Bonding Parameters ($b^{1/2}$), which are computed by using following formulae [20, 21]. The Nephelauxetic Ratio is given by

$$\beta' = \frac{v_g}{v_a} \quad (9)$$

where, v_a and v_g refer to the energies of the corresponding transition in the glass and free ion, respectively. The value of bonding parameter ($b^{1/2}$) is given by

$$b^{1/2} = \left[\frac{1-\beta'}{2} \right]^{1/2} \quad (10)$$

IV. RESULT AND DISCUSSION

A. XRD Measurement

Figure 1 presents the XRD pattern of the sample contain $-P_2O_5$ which is show no sharp Bragg's peak, but only a broad diffuse hump around low angle region. This is the clear indication of amorphous nature within the resolution limit of XRD instrument.

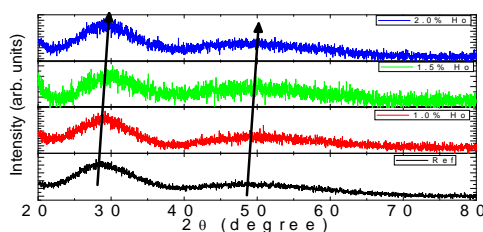


Fig. 1 X-ray diffraction pattern of ZLPCABP (HO) Glasses.

B. FTIR Transmission spectra

The FTIR spectrum of ZLPCABP glass samples are in the wave number range $450-1300\text{cm}^{-1}$ is presented in Fig.2 and the possible mechanism bands are tabulated in Table 2

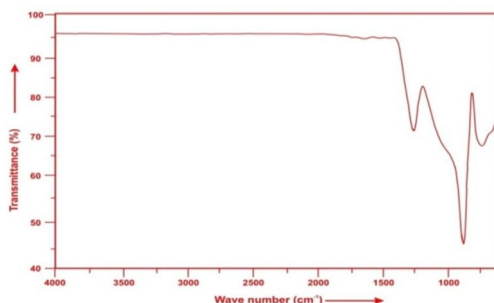


Fig. (2) FTIR spectrum of ZLPCABP HO (01) glass.

Table 2. Assignment of infrared transmission bands of ZLSPGBT HO (01) glass.

Peak position(cm ⁻¹)	Band Assignment
~740	symmetric stretching vibration of P-O-P bonding [22]
~890	Asymmetric stretching vibration of P-O-P bonds [22]
~1269	Asymmetric stretching vibration of P=O and O-P-O bonds [22]

C. Absorption Spectrum

The absorption spectra of Ho³⁺ doped ZLPCABP glass specimens have been presented in Figure 3 in terms of optical density versus wavelength. Twelve absorption bands have been observed from the ground state ⁵I₈ to excited states ⁵I₅, ⁵I₄, ⁵F₅, ⁵F₄, ⁵F₃, ³K₈, ⁵G₆, (⁵G₄, ³G₅), ⁵G₄, ⁵G₂, ⁵G₃, and ³F₄ for Ho³⁺ doped ZLPCABP glasses.

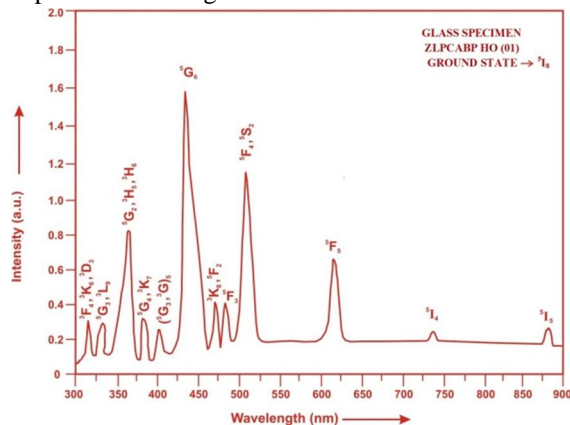


Fig. (3) Absorption spectrum of ZLPCABP HO (01) glass.

The experimental and calculated oscillator strength for Ho³⁺ ions in ZLPCABP glasses are given in Table 3.

Table 3: Measured and calculated oscillator strength (P_m×10⁺⁶) of Ho³⁺ ions in ZLPCABP glasses.

Energy level from ⁵ I ₈	Glass ZLPCABP (HO 01)		Glass ZLPCABP (HO1.5)		Glass ZLPCABP (HO02)	
	P _{exp.}	P _{cal.}	P _{exp.}	P _{cal.}	P _{exp.}	P _{cal.}
⁵ I ₅	0.53	0.25	0.50	0.25	0.46	0.24
⁵ I ₄	0.08	0.02	0.06	0.02	0.05	0.02
⁵ F ₅	3.78	2.84	3.74	2.81	3.71	2.79
⁵ F ₄	4.76	4.41	4.72	4.38	4.68	4.35
⁵ F ₃	1.70	2.46	1.67	2.44	1.63	2.43
³ K ₈	1.48	2.02	1.44	1.99	1.41	1.98
⁵ G ₆	26.68	26.60	25.45	25.39	24.69	24.67
(⁵ G ₄ , ³ G ₅)	3.96	1.71	3.92	1.68	3.87	1.67
⁵ G ₄	0.009	0.62	0.08	0.61	0.06	0.61
⁵ G ₂	5.98	5.64	5.94	5.42	5.91	5.28
⁵ G ₃	1.60	1.43	1.56	1.40	1.52	1.39
³ F ₄	1.38	4.21	1.35	4.16	1.30	4.12
r.m.s. deviation	1.1364		±1.1335		±1.1354	

Computed values of F₂, Lande' parameter (ξ_{4f}), Nephelauxetic ratio (β') and bonding parameter (b^{1/2}) for Ho³⁺ ions in ZLPCABP glass specimen are given in Table 4.

Table 4: F_2 , ξ_{4f} , β' and $b^{1/2}$ parameters for Holmium doped glass specimen.

Glass Specimen	F_2	ξ_{4f}	β'	$b^{1/2}$
Ho ³⁺	358.82	1258.16	0.9337	0.1821

In the Zinc Lithium Potassium Calcium Alumino Borophosphate glasses (ZLPCABP) Ω_2 , Ω_4 and Ω_6 parameters decrease with the increase of x from 1 to 2 mol%. The order of magnitude of Judd-Ofelt intensity parameters is $\Omega_2 > \Omega_6 > \Omega_4$ for all the glass specimens. The spectroscopic quality factor (Ω_4 / Ω_6) related with the rigidity of the glass system has been found to lie between 0.596 and 0.603 in the present glasses.

The values of Judd-Ofelt intensity parameters are given in

Table 5

Table 5: Judd-Ofelt intensity parameters for Ho³⁺ doped ZLPCABP glass specimens.

Glass Specimen	$\Omega_2(\text{pm}^2)$	$\Omega_4(\text{pm}^2)$	$\Omega_6(\text{pm}^2)$	Ω_4 / Ω_6
ZLPCABP (HO 01)	6.523	1.349	2.236	0.6033
ZLPCABP (HO1.5)	6.175	1.329	2.216	0.5997
ZLPCABP (HO 02)	5.967	1.314	2.205	0.5959

D. Excitation Spectrum

The Excitation spectrum of ZLPCABP (HO 01) glass has been presented in Figure 4 in terms of Excitation Intensity versus wavelength. The excitation spectrum was recorded in the spectral region 325–525 nm fluorescence at 545nm having different excitation band centered at 349,419, 452, 473and 486 nm are attributed to the 5G_3 , (5G , 3G)₅, 5G_6 , 3K_8 and 5F_3 transitions, respectively. The highest absorption level is 5G_6 and is at 452nm. So this is to be chosen for excitation wavelength.

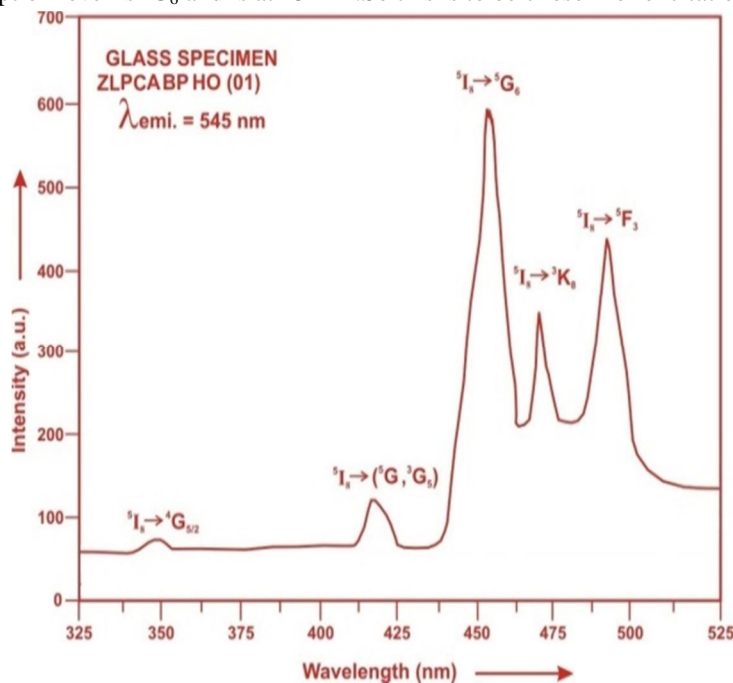


Fig. (4) Excitation spectrum of ZLPCABP HO (01) glass.

E. Fluorescence Spectrum

The fluorescence spectrum of Ho³⁺doped in zinc lithium potassium calcium alumino borophosphate glass is shown in Figure 5. There are eleven broad bands observed in the Fluorescence spectrum of Ho³⁺doped zinc lithium potassium calcium alumino borophosphate glass. The wavelengths of these bands along with their assignments are given in Table 6. The peak with maximum emission intensity appears at 2035 nm and corresponds to the ($^5I_7 \rightarrow ^5I_8$) transition.

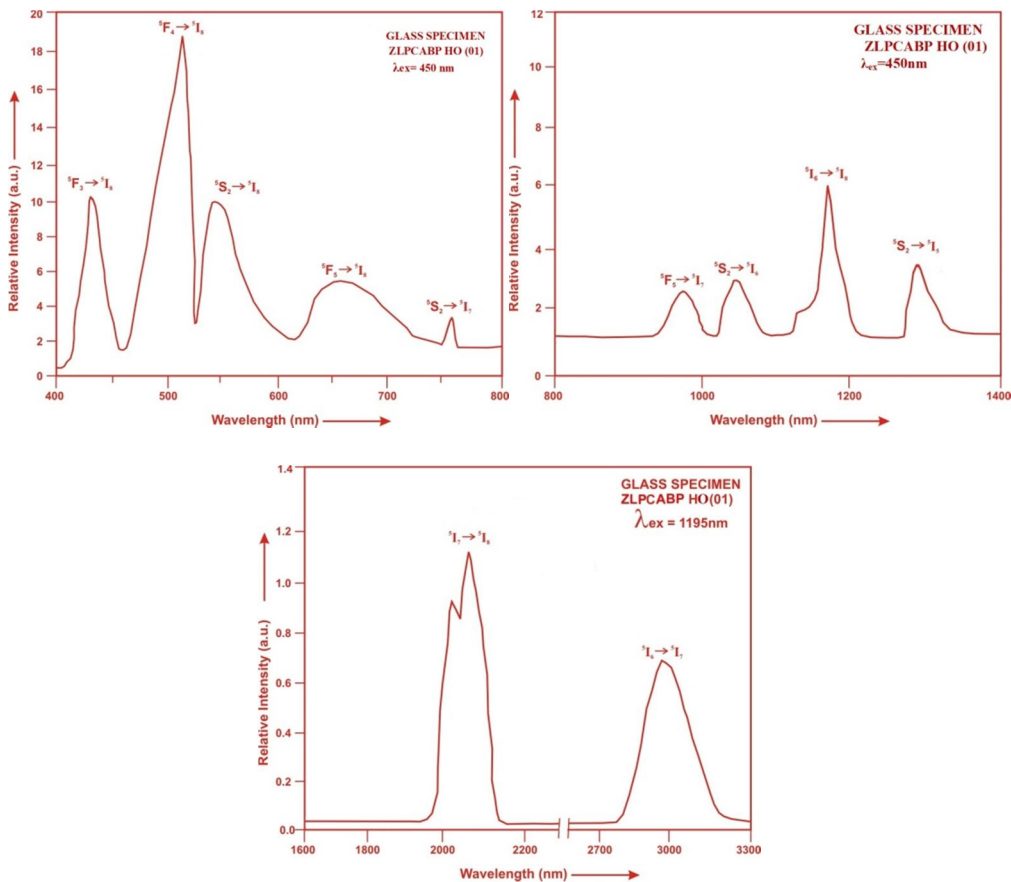


Fig. (5). Fluorescence spectrum of ZLPCABP HO (01) glass.

Table6: Emission peak wave lengths (λ_p),radiative transition probability (A_{rad}),branching ratio (β),stimulated emission cross-section(σ_p) and radiative life time(τ_R) for various transitions in Ho³⁺ doped ZLPCABP glasses.

Transition	ZLPCABP (HO 01)					ZLPCABP (HO 1.5)					ZLPCABP (HO 02)				
	λ_{max} (nm)	$A_{rad}(s^{-1})$	β	$\sigma_p (10^{-20} cm^2)$	$\tau_R(\mu s)$	$A_{rad}(s^{-1})$	β	$\sigma_p (10^{-20} cm^2)$	$\tau_R (\mu s)$	$A_{rad}(s^{-1})$	β	$\sigma_p (10^{-20} cm^2)$	$\tau_R (10^{-20} cm^2)$		
$^5F_3 \rightarrow ^5I_8$	435	4279.69	0.2487	0.607	5811.75	4246.91	0.2488	0.591	5857.41	4237.15	0.2491	0.574	5879.41		
$^5F_4 \rightarrow ^5I_8$	501	6781.86	0.3941	1.239		6729.21	0.3942	1.212		6699.42	0.3939	1.185			
$^5S_2 \rightarrow ^5I_8$	555	1785.43	0.1038	0.447		1773.94	0.1039	0.436		1768.64	0.1040	0.429			
$^5F_5 \rightarrow ^5I_8$	652	1926.53	0.1120	0.742		1909.56	0.1119	0.738		1900.11	0.1117	0.727			
$^5S_2 \rightarrow ^5I_7$	761	1355.22	0.079	1.140		1345.76	0.0788	1.119		1341.74	0.0789	1.110			
$^5F_5 \rightarrow ^5I_7$	995	450.69	0.026	1.235		445.12	0.0261	1.203		441.96	0.0260	1.173			
$^5I_6 \rightarrow ^5I_8$	1032	207.62	0.012	0.705		206.06	0.0121	0.685		205.33	0.0121	0.669			
$^5S_2 \rightarrow ^5I_5$	1195	237.67	0.014	1.236		235.61	0.0138	1.205		234.69	0.013	1.179			

$^5S_2 \rightarrow ^5I_6$	1310	63.29	0.0037	0.630	62.84	0.0037	0.612	62.64	0.0037	0.601
$^5I_7 \rightarrow ^5I_8$	2035	94.43	0.0055	4.784	93.56	0.0055	4.645	93.13	0.0055	4.535
$^5I_6 \rightarrow ^5I_7$	2925	24.09	0.0014	3.995	23.82	0.0014	3.908	23.69	0.0014	3.844

V. CONCLUSION

In the present study, the glass samples of composition (30-x)P2O5: 10ZnO: 10Li2O: 10K2O: 10CaO: 10Al2O3:20B2O3:xHo2O3. (where x =1, 1.5 and 2mol %) have been prepared by melt-quenching method. The value of stimulated emission cross-section (σ_p) is found to be maximum for the transition ($5I_7 \rightarrow 5I_8$) for glass ZLPCABP (HO 01), suggesting that glass ZLPCABP (HO 01) is better compared to the other two glass systems ZLPCABP (HO1.5) and ZLPCABP (HO 02). The large stimulated emission cross section in tellurite glasses suggests the possibility of utilizing these systems as laser materials. The FTIR of glasses revealed the presence of characteristic bonding vibrations of different functional groups

REFERENCES

- Othman, H., Elkholy, H., Cicconi, M.R., Palles, D., Ligny, D. de, Kamitsos, E.I., Moncke, Doris, Spectroscopic study of the role of alkaline earth oxides in mixed borate glasses-site basicity, polarizability and glass structure, *J. Non-Cryst. Solids*, 533, 1-11 (2020).
- Meena, S.L., Spectral and Upconversion Properties of Dy³⁺ ions doped Zinc Lithium Potassium borosilicate Glasses, *International Journal of Engineering Science Invention*, 11, 44-49 (2022).
- Kashif, I., Ratep, A. and Ahmed, S., Spectroscopic properties of lithium borate glass containing Sm³⁺ and Nd³⁺ ions, *Int. J. of Adv. in App. Sci.* 9(3), 211-219 (2020).
- Shwetha, M., Eraiah, B., Influence of Dy³⁺ ions on the physical, thermal, structural and optical properties of lithium zinc phosphate glasses, *J. Non-Cryst. Solids*, 555, 1-10 (2021).
- Liu, L., Xing, J., Shang, F., Chen, G., Structure and up-conversion luminescence of Yb³⁺/Ho³⁺ co-doped fluoroborate glasses, *Opt. Comm.* 490, 1-6 (2021).
- Meena, S.L. Spectral and Raman Analysis of Er³⁺ doped Ytterbium Zinc Lithium Sodalime Magnesium Borophosphate Glasses, *In. J. Inn. Res. Sci., Eng. and Tech.*, 12, 10915-24 (2023).
- M.A. Khan, R.J. Amjad, M.A. Ahmad, A. Sattar, S. Hussain, S. Yasmeen, M.R. Dousti, Structural and optical study of erbium doped borophosphate glass. *Optic*, 206, 16370 (2020)
- Z. Zhao, B. Zhang, Y. Gong, Y. Ren, M. Huo, Y. Wang, Concentration effect of Yb³⁺ ions on the spectroscopic properties of high-concentration Er³⁺/Yb³⁺ co-doped phosphate glasses. *J. Mol. Struct.* 1216, 128322 (2020).
- H. Largot, K.E. Aiadi, M. Ferid, S. Hraiech, C. Bouzidi, C. Charny, Spectroscopic investigation of Sm³⁺ doped phosphate glasses: Judd-Ofelt analysis, *Phys. B Condens. Matter*, 552, 184-189 (2019).
- Vijay, N. and Jayasankar, C.K., Structural and spectroscopic properties of Eu³⁺ doped zinc fluorophosphates glasses, *J. Mol. Struct.*, 1036, 42-50 (2013).
- Marzouk, M.A., ElBatal, H.A., Hamdy, Y. M. and Ezz-Eldin, F.M., Collective Optical, FTIR and Photoluminescence Spectra of CeO₂ and/or Sm₂O₃-Doped Na₂O-ZnO-P₂O₅ Glasses. *Int. J. Opt.* 6527327, 1-11 (2019).
- Kumar, G.R. and Rao, C.S., Influence of Bi₂O₃, Sb₂O₃ and Y₂O₃ on optical properties of Er₂O₃-doped CaO-P₂O₅-B₂O₃ glasses, *Bull. Mater. Sci.* 43:71, 1-7 (2020).
- Shailajha, S., Geetha, K. and Vasantharani, P., Spectral studies on CuO in sodium-calcium borophosphate glasses. *Bull. Mater. Sci.*, 39(4), 1001-1009 (2016).
- Karabulut, M., Popa, A., Borodi, G. and Stefan, R., An FTIR and ESR study of iron doped calcium borophosphate glass-ceramics. *Journal of Molecular Structure*, 1101, 170-175 (2015).
- Guan, P.X., Yew, E.T., Ming, L.P., Shamsuri, W.N.W., Hussin, R. Structural and Luminescence Study of Rare Earth and Transition Metal Ions Doped Lead Zinc Borophosphate Glasses, *Adv. Mat. Res.* 895, 280-283 (2014).
- Gorller-Walrand, C. and Binnemans, K., Spectral Intensities of f-f Transition. In: Gshneidner Jr., K.A. and Eyring, L., Eds., *Handbook on the Physics and Chemistry of Rare Earths*, Vol. 25, Chap. 167, North-Holland (1998). Amsterdam, 101-264.
- Sharma, Y.K., Surana, S.S.L. and Singh, R.K. Spectroscopic Investigations and Luminescence Spectra of Sm³⁺ Doped Soda Lime Silicate Glasses. *Journal of Rare Earths*, 27, 773-780 (2009).
- Judd, B.R., Optical Absorption Intensities of Rare Earth Ions. *Physical Review*, 127, 750-761 (1962).
- Ofelt, G.S., Intensities of Crystal Spectra of Rare Earth Ions. *The Journal of Chemical Physics*, 37, 511 (1962).
- Sinha, S.P., Systematics and properties of lanthanides, Reidel, Dordrecht. 1-8 (1983).
- Krupke, W.F., *IEEE J. Quantum Electron* QE, 10, 450 (1974).
- Babu, S., Prasad, V.R., Rajesh, D., Ratnakaram, Y.C. Luminescence properties of Dy³⁺ doped different fluoro-phosphate glasses for solid state lighting applications. *J. Mol. Struct.* 1080, 153-160 (2015).



10.22214/IJRASET



45.98



IMPACT FACTOR:
7.129



IMPACT FACTOR:
7.429



INTERNATIONAL JOURNAL FOR RESEARCH

IN APPLIED SCIENCE & ENGINEERING TECHNOLOGY

Call : 08813907089  (24*7 Support on Whatsapp)